

A WINTER COVER CLASSIFICATION OF LOWER NAKDONG RIVER REGION USING JERS-1 OPS DATA

Choen Kim^(*)
Associate Professor
Department of Forest Resources
Kookmin University
Seoul 136-702, KOREA

Commission VII, Working Group 1

KEY WORDS : Land Cover Classification, Spectral Angle Mapper, Maximum Likelihood Classification, Vegetation Indexes, Bidirectional Reflectance Effects, Geometric Illumination Conditions, JERS-1 OPS Multispectral Data

ABSTRACT :

Spaceborne multispectral data have been used cost-effectively for monitoring of land surfaces. It is the purpose of this study to evaluate new methods for land cover classification of satellite imagery influenced by illumination conditions due to terrain irregularities. Low solar elevations cause strong shadow effects in mountainous terrain. In order to examine the effect of bidirectional reflection on the reflected radiance response of the JERS-1 OPS bands, the NDVI and TVI were analyzed for differential shading. These geometric illumination effects hinder accurate land use classification. This paper shows how the effects of differential shading on the classification of vegetation could be reduced through the use of the Spectral Angle Mapper(SAM) algorithm. This method proved better than layered classification logic or rule-based expert systems and fuzzy classification with nonparametric priors. In addition, maximum likelihood classification was used to distinguish between two different water properties (freshwater and salt water) on the images. These areas were not influenced by topographic effects. The spectral angle mapper classification method produced seven land cover classes in the lower Nakdong River region : forest, urban, winter agricultural area, reed vegetation, barren(rock & sands), river(freshwater) and sea (salt water), and an unclassified category which indicated shadow areas in the mountainous forests.

1. INTRODUCTION

Until recently, the incorporation of ancillary data and fuzzy logic have been used for improving the classification accuracy of remotely sensed data. However, these methods are applied only to the specific information extraction, require a more complex hierarchical process than conventional supervised classification method, and are more expensive (Wang & Civco, 1992 ; Maselli et al., 1995 ; Jensen, 1996).

The Spectral Angle Mapper (SAM) method allows single-step matching of pixel spectra to reference spectra in n-dimensional spectral space. The effects of shadow on the final classification image can essentially be eliminated using this technique.

Moreover, this method can also be applied to discrimination of vegetated surfaces which reflect incident solar radiation anisotropically. The recently observed directionality of reflectance in vegetation could be divided into forward, nadir and back scatter directions (Deering et al., 1992 ; Hanan et al., 1995).

These considerations led to the initiation of a research project to determine if multispectral data acquired by the Japanese Earth Resource Satellite-1 Optical Sensor (JERS-1 OPS) could be used for classifying land-use and vegetative cover type in the lower Nakdong River region. It is anticipated that JERS-1 OPS data will provide information on regional land cover changes for environmental and ecological monitoring.

The objectives of this paper are :

- 1) To develop a winter land cover classification using the Visible and Near-Infrared (VNIR) bands of JERS-1 OPS.
- 2) To analyze the vegetation indexes (NDVI and TVI) for geometric illumination conditions influenced by topography (slope, aspect and elevation) and shadows (solar elevation and azimuth angle).
- 3) To assess the accuracy of the SAM classification in comparison with the maximum likelihood method.
- 4) To identify tidal spread in Nakdong River, and the boundaries of the freshwater in the coast.

2. STUDY AREA AND DATA

The study area includes the western part of Pusan, and is situated at approximately 35° 12' North latitude, 128° 52' East longitude. It is approximately 8027 hectares in size. The area is divided into a steep mountain portion a delta plain portion, and a river and coastal sea portion. The last portion has the characteristics of upstream tidal currents and dispersion of the Nakdong River water. The flat portion of the area consist mostly of rice fields in summer and dry field agricultural activities (including Vinyl(Green) house farming) in winter, urban buildings zone, and a wetland with reed vegetation.

Within the area, the test sites which comprise the homogeneous forest canopies of mountainous Morundai (A) and the homogeneous hanging reeds near Shinho village (B) were specially selected for analysis of the bidirectional effects.

The dominant overstory tree species in site A is pine (*Pinus thunbergii* Parl.), and the understory trees are oaks (*Quercus acutissima* Carruth, *Quercus aliena* Bl. and *Quercus*

(*) He will be a visiting professor at the Department of Forest Resources at the University of Idaho, Moscow, ID 83844-1133, USA, until August 1996.

dentata Thunb.). Site B is a typically flat region of reed vegetation (*Phragmites communis* Trim.) in the Nakdong River estuary. The estuary is well-known as winter habitat for migratory birds and is characterized largely by sandbars and sand dunes.

JERS-1 OPS data for the study area were obtained on 26 December 1992, 11:23 A.M. with a solar elevation of 28.9° and a sun azimuth of 160.8°. The system correction which has been performed by RESTEC (Remote Sensing Technology Center) of Japan was made up to BSQ Level 2. The OPS VNIR subsystem has two bands in the visible region (band 1: 0.52 - 0.60 μm, band 2: 0.63 - 0.69 μm), and two bands in the near infrared region (band 3, 4: 0.76 - 0.86 μm) including one band for stereoscopic view (forward looking) with a ground resolution of 18.3m x 24.2m.

3. METHODOLOGY

A total of 137 sample polygons of mountainous forest were selected within the study area image for four different aspects: N(316° - 45°), E(46° - 135°), S(136° - 225°), and W(226° - 315°). The digital numbers of three bands (green, red and near infrared) were measured for each of these polygons. In order to minimize the heterogeneity of the samples and to explore bidirectional effects on different canopy types resulting from vegetation and topography the normalized difference vegetation index (NDVI) and the transformed vegetation index (TVI) were investigated.

In this study the NDVI was calculated as $(OPS\ 3 - OPS\ 2) / (OPS\ 3 + OPS\ 2)$ and the TVI was calculated as $[(OPS\ 3 - OPS\ 2) / (OPS\ 3 + OPS\ 2) + 0.5]^{1/2}$, where OPS 2 and OPS 3 are the DN values in OPS band 2 and 3, respectively.

For most vegetated surfaces with variation in reflectance directionality the obtained vegetation indices were unable to discriminate the detailed classes for land cover when the change rates of vegetation indices against for different aspects were larger than the change rates of reflectance values for different aspects caused by the effect of shadows due to steep slopes and low solar elevation. The maximum-likelihood classification algorithm was also unable to classify the mountainous areas accurately.

On the other hand, water surfaces were flat so that those satellite images could be classified for water properties and qualities with maximum likelihood method.

During the course of this study I found that the effects of shadows on the classification of JERS-1 OPS images could be reduced through the SAM algorithm. The SAM algorithm determines the spectral signature similarity between the representative spectral mean DN values calculated from the training field pixels and the spectral DN values derived from each pixel in the image through the spectral angle differences (angular distance in radians) between their vector directions in n-dimensional (band) space. A more detailed mathematical description of the algorithm, concepts and applications of the program are described in CSES and CIRES(1992), Research Systems, Inc.(1995), and Yuhua and Goetz(1993).

The OPS VNIR data were processed and analyzed using the Environment for Visualizing Image (ENVI) image analysis and the Arc/Info and ArcView GIS software on a Sun sparc 10/51 workstation in the Department of Forest Resources Remote Sensing Laboratory at Kookmin University, Seoul, Korea.

4. RESULTS AND DISCUSSION

4.1 Directionality of Vegetation Indexes and Spectral Reflectances

The weighted mean values of the spectral digital numbers and vegetation indices for four slope orientations obtained through 137 sample polygons are given in Table 1. In the mountainous forests at a sun elevation of 28.9° and a sun azimuth of 160.8°, the spectral reflectance(DN) values decrease in the order of south, east, west and north(Figure 1).

But the magnitude order of NDVI is neither consistent with that of TVI nor of the DNs, and the change rates of NDVI values for different directions are larger than those of TVI values.

These phenomena can be explained by the heterogeneity of the samples and the variation of bidirectional effects. Table 2 presents the variation of vegetation indexes due to bidirectional effects in the homogeneous forest canopy structure of the mountainous site A when compared to the vegetation indexes of reeds vegetation on the flat site B. Since the both VI values of site B are similar for all four reflected directions these normalized relationship methods can be used as a winter cover monitoring parameter on flat terrain, regardless of illumination under low sun elevation condition.

Due to the strong illumination variation in mountain area with steep slopes the obtained vegetation indexes were also stratified by aspect against the four reflective directions.

4.2 Spectral Signatures Analysis

As pointed out in the above result, the spectral reflectance characteristics of land covers of the study area could be limited to case of flat terrains because it is difficult to refine the correction model for topographic effects. Figure 2 shows different spectral responses from nadir views of OPS-VNIR data (except band 4) for the ground in flat terrains.

When compared to the other spectral DN values, land cover classes of reeds vegetation and sand dune bordered on the river and estuary low reflectance values in the green, red, and near-infrared band. This phenomenon was influenced by high water absorption. The spectral signature distinctiveness between cover type sand dune and rock & sands were also related to water content which altered the scatter directions of the reflectances.

Typically spectral signature similarity for spectral reflectance curves and separability between vegetated and non-vegetated cover types on the images can be determined through the use of NDVI. This phenomenon is evident in the NDVI values for the classes reeds vegetation and fallow & arable farming shown in Table 3.

For water surfaces the VNIR data acquired by an off-nadir optical system with a Charge Coupled Device(CCD) are relatively insensitive to geometric illumination conditions compared with whiskbroom scanning.

Therefore, the spectral reflectance responses and derived vegetation indices could be used to estimate the quality of water, monitor the water pollution sources and the turbid water induced by tide in Nakdong River estuary.

Figure 3 shows the spectral digital numbers and vegetation indexes obtained from VNIR values over water bodies in Nakdong River and the coastal zone.

The spectral reflectances of freshwater and salt water decreased as wavelength increased.

Additionally, the decreasing rate of freshwater reflectances was greater than that of the salt water reflectances.

Therefore, red and near-infrared reflectances of the river water body were higher than those of the sea water body (see Figure 3 (B)).

This may be due to high turbidity causing high reflectance and low absorption in red and near-infrared bands.

It should be noted that the higher vegetation indexes for the river were related to higher suspended solid concentrations present compared to the sea water (see Figure 3 (A)) because yellow substances absorb mainly in blue region of the spectrum (Tassan, 1988). As a consequence, the spectral signatures of water bodies vary with turbidity and its composition so that OPS VNIR data are useful for monitoring of water quality.

4.3 Spectral Angle Mapper and Maximum Likelihood Classification

With the limitation of flat water surfaces the supervised classification method using a maximum likelihood decision rule provided the best display of the location and movement of both freshwater and salt water. Because the classified pixels have the highest probability, the resulting classes are sufficiently accurate for the mapping of the diffusion Nakdong River water into the coastal sea, and also its influences on the adjacent coastal environments (Figure 4).

As shown in Figure 4 maximum likelihood classification shows promise in detection of water properties.

Finally, a major advantage of SAM algorithm is that it is available for discriminating the given seven classes within shaded polygons by using as an additional parameter the measure of maximum acceptable angle between spectra vectors, because the decision rule of spectral angle depends only on the direction of the spectra, not their length (Research Systems, 1995). The site-specific accuracy assessment that compared and ground truth data with a GIS supporting verification the results of SAM classification are presented in Table 4.

The SAM classification was conducted using an additional parameter measured in "Maximum Angle (radians)". To evaluate the effect of this parameter unclassified areas were selected, and compared to the corresponding areas on shaded relief image on the color composite scene. When unclassified mountain areas were added to the forest class the resulting value was very similar to the sample value.

The ground truth data collected at the end of December, 1994 were used for the validation of the proposed land cover classes. Also during the study I found that the GIS supported in-situ analysis could be used for detecting the land cover changes of the classified image data in agricultural areas and wildlife and bird sanctuaries related mainly to human impact.

The identification of shadow areas (mainly termed unclassified) was accomplished through visual interpretation, and could be exactly displayed on the processed images.

5. CONCLUSION

1. The SAM method produced a more accurate land cover classification of areas with steep slopes, various aspects and low solar angles than conventional classification

methods.

2. The spectral digital numbers and vegetation indexes of mountainous forest areas were higher for aspects facing the sun than for aspects away from sun under low sun elevation condition.
3. The spectral digital numbers and vegetation indexes for the flat terrains could be used as ecological and environmental parameters, regardless of geometric illumination conditions.
4. The supervised classification of water surface was useful for monitoring changing water properties in estuarine and coastal areas.

ACKNOWLEDGEMENTS

This work was financially supported by the Korea Science and Engineering Foundation under Contract KOSEF 941-1300-008-1 with the Kookmin University.

NASDA (National Space Development Agency) of Japan provided the JERS-1 OPS data, whose ownership belong to MITI (Ministry of International Trade and Industry) / NASDA.

The author wishes to thank Dr. Jerry Korol at the Department of Forest Resources, University of Idaho for his help in reviewing the manuscript.

REFERENCES

- Center for the Study of Earth from Space (CSES) and Cooperative Institute for Research in Environmental Sciences (CIRES), 1992. SIPS User's guide : Spectral image processing system, version 1.2. University of Colorado, Boulder, pp.16-29.
- Deering, D. W., Middleton, E. M., Irons, J. R., Blad, B. L., Walter-shea, E. A., Hays, C. J., Walthall, C. L., Eck, T. F., Ahmad, S. P. and B. P. Banerjee, 1992. Prairie grassland bidirectional reflectances measured by different instruments at the FIFE site. *J. Geophys. Res.*, 97, pp. 18887-18904.
- Hanan, N. P., Brown de Colstoun and S. D. Prince, 1995. Estimation of canopy photosynthetically active radiation (PAR) interaction using bidirectional aircraft reflectance measurements of the HAPEX-sahel bush fallow subsite. In : *Proc. of IGARSS'95 Symposium, Firenze*, pp. 1299-1301.
- Jensen, J.R., 1996. *Introductory Digital Image Processing : A remote sensing perspective*. Prentice Hall, Upper Saddle River, NJ, pp 240-247.
- Maselli, F., Conese, C., Filippis T. D. and S. Norcini, 1995. Estimation of forest parameters through fuzzy classification of TM data. *IEEE Trans. Geosci. Remote Sensing*, 33(1), pp 77-83.
- Research Systems, Inc., 1995. *ENVI Version 2.0 Tutorial*. Boulder, Colorado.
- Tassan, S., 1988. The use of Thematic Mapper for coastal water analysis. In : *International Archives of Photogrammetry and Remote Sensing, Kyoto, Japan, Vol. 16*.
- Wang, Y. and D. L. Civco, 1992. Post-classification of misclassified pixels by evidential reasoning : A GIS approach

for improving classification accuracy of remote sensing data. In : International Archives of Photogrammetry and Remote Sensing , Washington D. C., USA, Commission VII, pp. 80-86.

Yuhas, R. H. and A. F. H. Goetz. 1993. Comparison of airborne (AVIRIS) and spaceborne (TM) imagery data for discriminating among semi-arid landscape endmembers. In : Proc. of Ninth Thematic Conference on Geologic Remote Sensing, Pasadena, USA, pp. 503-511.

Table 1. Weighted mean values of the spectral DN and VI influenced by bidirectional effects

Direction	Digital Number			Vegetation Index	
	Green	Red	IR	NDVI	TVI
North	47.9	39.7	50.9	0.107	0.776
South	60.0	60.4	79.4	0.173	0.797
East	55.7	52.4	73.5	0.156	0.808
West	51.0	45.7	53.1	0.058	0.744

Table 2. Vegetation indices of four different directions in testsite A (mountainous forest) and in testsite B (reeds vegetation on flat terrain).

Direction	Site A (Morundai)		Site B (near Shinho)	
	NDVI	TVI	NDVI	TVI
North	0.049	0.741	-0.099	0.633
South	0.374	0.935	-0.101	0.631
East	0.291	0.889	-0.107	0.627
West	-0.211	0.538	-0.102	0.631

Table 3. Normalized Difference Vegetation Index (NDVI) values for different land cover types on flat terrains.

	Reeds vegetation	Sand dune	Urban	Vinyl(Green) house	Rock & Sands	Fallow & Arable farming
NDVI	0.011	-0.110	-0.097	-0.025	-0.071	0.077

Table 4. Comparison of the SAM classification with GIS supported in-situ analysis in percentage of the classified of the classified pixels.

Class	Number of Pixels	Cover %	Number of Re.Sample	Cover %
Unclassified	111039	9.08	-	-
Forest	378379	18.87	39	28.06
Urban	81991	6.70	10	7.19
Winter Agricultural	232493	19.01	16	11.51
Vinyl(Green)house	-	-	8	5.75
Barren	6046	0.49	-	-
Reeds Vegetation	54168	4.43	5	3.60
River	69881	5.71	5	3.60
Sand dune	-	-	1	0.72
Coastal sea	436588	35.70	55	39.57
Total	1222940	100	139	100

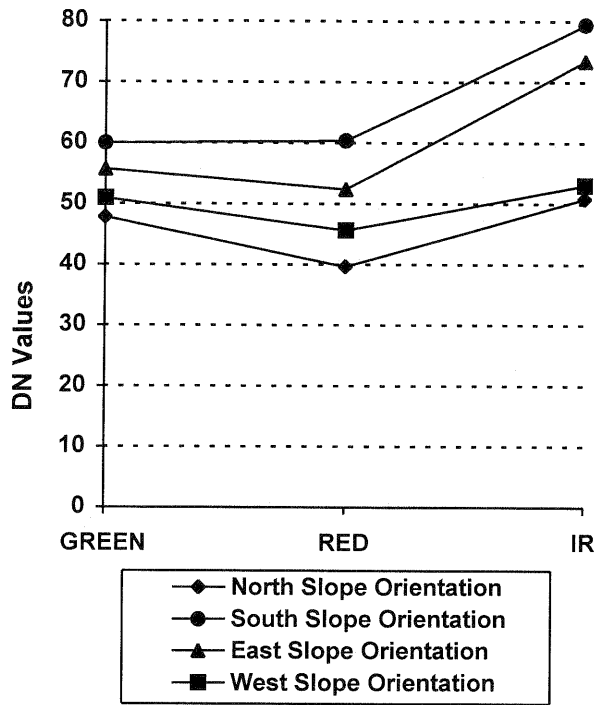


Figure 1. Spectral bidirectional reflectance characteristics of mountainous forests for four different aspects (see Table 1 for DN's)

	<i>Reeds vegetation</i>	<i>Sand dune</i>	<i>Urban</i>	<i>Vinylhouse</i>	<i>Rock & Sands</i>	<i>Fallow & Arable farming</i>
IR	65.11	52.50	63.63	90.98	104.76	85.94
R	63.68	65.50	77.27	95.55	120.66	73.59
G	67.11	67.80	77.09	87.27	103.02	71.00

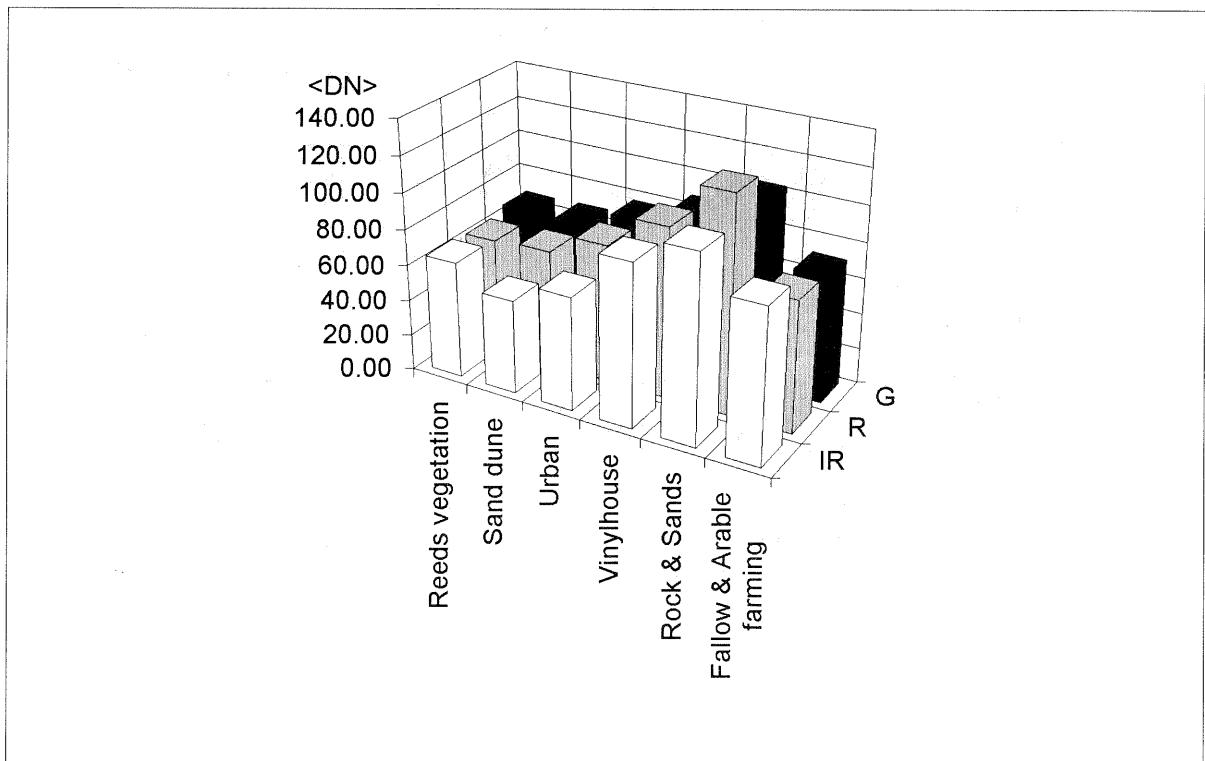


Figure 2. Digital number (DN) of three bands for different winter cover types on flat terrains

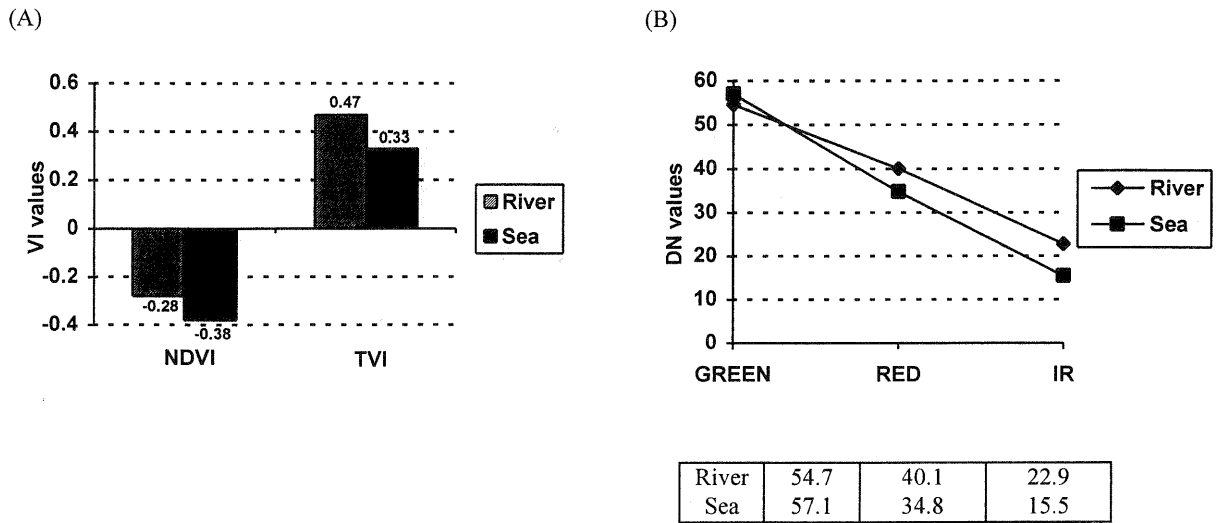


Figure 3. Vegetation indexes (A) and spectral DNs (B) over a freshwater area of 12.0257sq km and salt water area of 136.2918 sq km.

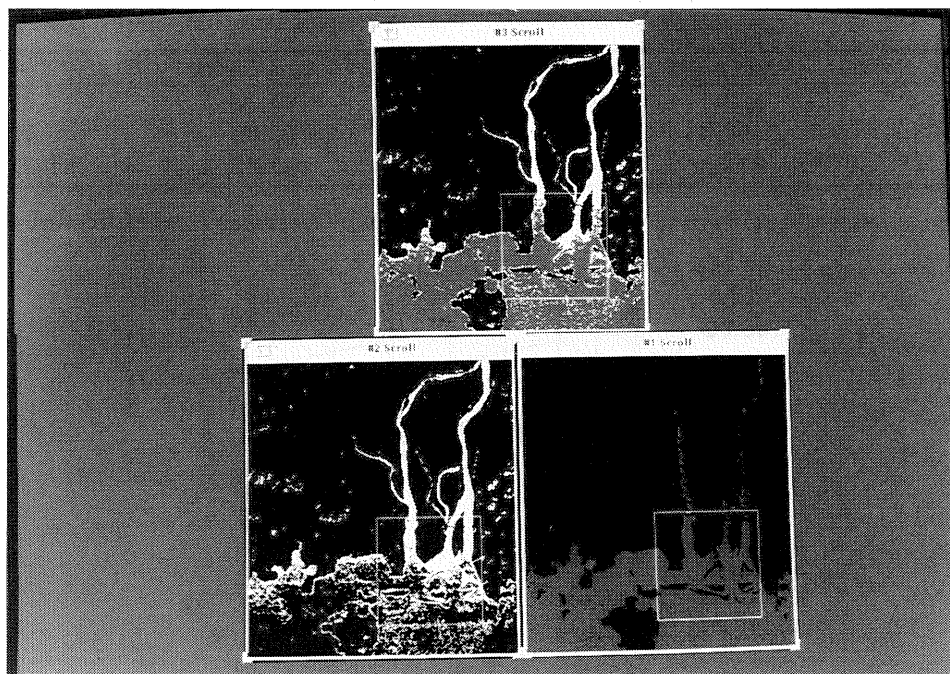


Figure 4. Maximum likelihood Classification images of water bodies on the Nakdong River delta near Pusan in Korea. (A) Incursion of salt water from the estuary, see # 3 above. (B) Dispersion of Nakdong River freshwater influenced by neritic current, see # 2 bottom left. (C) Tidal spread inside the Nakdong River, see #1 bottom right.